Addition of a fast GC to SIFT-MS for analysis of individual monoterpenes in mixtures

Michal Lacko[1,2], Nijing Wang[3], Kristýna Sovová[1], Pavel Pásztor[1], Patrik Španěl[1]

[1]The Czech Academy of Science, J. Heyrovský Institute of Physical Chemistry, Dolejškova 2155/3, 182 23 Prague, Czech Republic

[2]Faculty of Mathematics and Physics, Charles University in Prague, Ke Karlovu 3, 121 16 Prague, Czech Republic

[3]Air Chemistry Department, Max-Planck-Institut für Chemie, Hahn-Meitner-Weg 1, 55128 Mainz, Germany

Correspondence to: Michal Lacko (michal.lacko@jh-inst.cas.cz)

Abstract. Soft chemical ionization mass spectrometry (SCI-MS) techniques can be used to accurately quantify volatile organic compounds (VOCs) in air in real time; however, differentiation of isomers still represents a challenge. A suitable pre-separation technique is thus needed, ideally capable of analyses in a few tens of seconds. To this end, a bespoke fast GC with an electrically heated 5 m long metallic capillary column was coupled to selected ion flow tube mass spectrometry (SIFT-MS). To assess the performance of this combination a case study of monoterpene isomer ($C_{10}H_{16}$) analyses was carried out. The monoterpenes were quantified by SIFT-MS using H_3O^+ reagent ions (analyte ions $C_{10}H_{17}^+$, *m/z* 137, and $C_6H_9^+$, *m/z* 81) and NO^+ reagent ions (analyte ions $C_{10}H_{16}^+$, *m/z* 136, and $C_7H_9^+$, *m/z* 93). The combinations of the fragment ion relative intensities obtained using H_3O^+ and NO^+ were shown to be characteristic for the individual monoterpenes. Two non-polar GC columns (Restek Inc.) were tested: the advantage of MXT-1 was shorter retention whilst the advantage of MXT-Volatiles was better separation. Thus it is possible to identify components of a monoterpene mixture in less than 45 s by the MXT-1 column and to separate them in less than 180 s by the MXT-Volatiles column. Quality of separation and sensitivity of present technique (LOD ~16 ppbv) was found to be inferior compared to commercially available fast-GC solutions coupled with proton transfer reaction mass spectrometry (PTR-MS, LOD ~1 ppbv) due to the limited sample flow through the column. However, using combinations of two reagent ions improved identification of monoterpenes not well resolved in the chromatograms. As an illustrative example, headspace of needle samples of three conifer species was analysed by both reagent ions and with both columns showing that mainly α-pinene, β-pinene and 3-carene were present. The system can thus be used for direct rapid monitoring of monoterpenes above 20 ppbv. Limitation of the sensitivity due to the total sample flow can be improved using a multicolumn pre-separation.

1 Introduction

Standard analytical methods used to identify and quantify volatile organic compounds (VOCs) in air, such as thermal desorption gas chromatography mass spectrometry (TD-GC-MS), are often time consuming and cannot be used to investigate temporal changes in chemically evolving systems. In contrast, soft chemical ionization mass spectrometry (SCI-MS)

1

techniques, such as selected ion flow tube mass spectrometry (SIFT-MS) (Smith and Španěl, 2011a; Španěl et al., 2006) and proton transfer reaction mass spectrometry (PTR-MS) (Lindinger et al., 1998; Ellis and Mayhew, 2013; Smith and Španěl, 2011b) represent well-established real time tools to analyse a wide variety of VOCs in ambient air (Amelynck et al., 2013; de Gouw and Warneke, 2007; Malásková et al., 2019; Rinne et al., 2005; Schoon et al., 2003) and in headspace of biological samples (Shestivska et al., 2015; Shestivska et al., 2011; Shestivska et al., 2012). The advantage of SIFT-MS and PTR-MS lies in the possibility of online, real-time analysis obviating sample collection and pre-concentration of VOCs. In these techniques, defined reagent ions (usually H_3O^+, NO^+ or $O_2^{+\bullet}$) interact with trace VOCs present in gas samples introduced into a flow tube or a flow/drift tube. The chemical ionisation reactions that produced analyte ions are variously proton transfer, adduct ion formation, charge transfer and hydride ion transfer, principally depending on the type of reagent ions used. This ion chemistry has been thoroughly reviewed in a number of publications (Smith and Španěl, 2005). These ion-molecule reactions are not greatly exothermic and so few product (analyte) ions are produced in each reaction, often just one or two, that can be readily identified. However, chemically similar molecules with the same atomic composition (structural isomers) usually produce identical analyte ions with similar branching ratios and therefore the neutral analyte molecules cannot be easily differentiated using SCI-MS alone (Smith et al., 2012). However, the reactions of the isomeric molecules may have different rate coefficients with the different reagent ions and lead to product ions at recognisably different branching ratios depending on their molecular geometry (Jordan et al., 2009; Pysanenko et al., 2009; Španěl and Smith, 1998; Wang et al., 2003). So the concurrent use of the available reagent ions in SIFT-MS analysis can sometimes be used to analyse and identify particular isomers.

Monoterpenes, mostly emitted from plants, are very important biogenic volatile organic compounds (BVOCs) in the atmosphere. Due to their high reactivity with atmospheric oxidants such hydroxyl radicals (OH•), monoterpenes reactions can lead to tropospheric ozone (O_3) accumulation as well as to secondary organic aerosol formation, which can affect human health and contribute to global climate change (Chameides et al. (1992); Fehsenfeld et al. (1992); Kulmala et al. (2004)). Although all monoterpenes comprise two isoprene units and have the same molecular formula, $C_{10}H_{16}$, their reactivity (or lifetime) for reaction with OH• and O_3 widely varies from minutes to days (Atkinson and Arey, 2003) (See Table 1). The values of the net BVOC/OH• reactivity measured in rainforests have been found to be higher than expected, which could be attributed to undetected monoterpenes or sesquiterpenes (Nolscher et al., 2016). Therefore, it is important to identify and individually quantify these BVOCs at their ambient trace levels.

Quantitative measurement of monoterpenes is often problematic due to the problems with stability of monoterpene mixtures in certified gas standards (Rhoderick and Lin, 2013). Therefore, fresh individual monoterpene standards or monoterpene mixtures are prepared from liquid standards. To determine an accurate instrument sensitivity to individual monoterpenes, the relative abundance of monoterpene isomers must be known (de Gouw et al., 2003).

Table 1. Monoterpenes included in the present study listed together with their atmospheric lifetimes and reactivities.

Compound	Lifetime for reaction with a OH[b] / O3[c]	Chemical lifetime[d] Day	Night	Rate constant of O3[e]	Rate constant of OH[f]
α-pinene	2.6 hrs / 4.6 hrs	2-3 hrs	5-30 min	8.7	5.45 ± 0.32
β-pinene	1.8 hrs / 1.1 day	2-3 hrs	5-30 min	1.5	7.95 ± 0.52
Camphene	2.6 hrs / 18 day	nd	nd	9.0[g]	5.33[g]
Myrcene	39 min / 50 min	40-80 min	5-20 min	49	21.3 ± 1.6
3-carene	1.6 hrs / 11 hrs	nd	nd	3.8	8.70 ± 0.43
R-limonene	49 min / 2.0 hrs	40-80 min	5-20 min	21	16.9 ± 0.5
α-terpinene	23 min / 1 min	< 5 min	< 2 min	870	36.0 ± 4.0
γ-terpinene	47 min / 2.8 hrs	nd	nd	14	17.6 ± 1.8

[a] taken from Atkinson (Atkinson and Arey, 2003) unless noted otherwise.

[b] Assumed OH radical concentration: 2.0×10^6 molecule cm^{-3}, 12-h daytime average.

[c] Assumed O$_3$ concentration: 7×10^{11} molecule cm^{-3}, 24-h average.

[d] Lifetimes are estimated in relation to [NO$_3$] = 10 ppt, [O$_3$] = 20 ppb for night; and [OH] = 10^6 molecules per cm^3, [O$_3$] = 20 ppb for day light conditions. (Kesselmeier and Staudt, 1999) (unless noted otherwise)

[e] Rate constants (in units of 10^{-17} cm^3 molecule^{-1} s^{-1}) for the gas-phase reactions of O$_3$ with a monoterpenes have been determined at 296 ± 2 K and 740 torr total pressure of air or O$_2$ using a combination of absolute and relative rate techniques. (Atkinson et al., 1990) (unless noted otherwise)

[f] Rate constants (in units of 10^{-11} cm^3 molecule^{-1} sec^{-1}) for the gas-phase reactions of the OH radical with monoterpenes have been determined in one atmosphere of air at 294 ± 1 K. (Atkinson et al., 1986) (unless noted otherwise)

[g] Rate constants of k(OH + isoprene) = 1.01×10^{-10} cm^3 molecule^{-1} s^{-1}. O$_3$ reaction rate constants determined in 10^{-19} cm^3 molecule^{-1} s^{-1} units. OH radical reaction rate constants determined in 10^{-11} cm^3 molecule^{-1} s^{-1} units. (Atkinson et al., 1990)

nd – no data

Gas chromatography mass spectrometry (GC-MS) coupled with pre-concentration techniques has been developed to successfully identify and quantify different atmospheric monoterpenes (Janson, 1993; Räisänen et al., 2009; Song et al., 2015). However, the requirements of pre-concentration and long cycle time (more than 1h) are obviously unsuitable for real-time measurements.

A promising approach to the near real time analysis of isomeric molecules is to combine both SCI-MS and fast GC methods. Pre-separation provided by fast GC involves short columns with thin active layers, fast temperature ramps, fast injection systems and time resolutions below 5 min (Matisová and Dömötörová, 2003). Materic et al. (Materić et al., 2015) established a system using PTR-MS coupled with a fast GC to detect individual monoterpenes and achieved the separation of six most common monoterpenes at a limit of detection down to 1 ppbv. Pallozzi et al. then compared a fastCG-PTR-ToF-MS system

with traditional GC-MS methods, discussing the limitations of the fast GC setup on some BVOCs emitted from plants, including monoterpenes (Pallozzi et al., 2016). SIFT-MS is also widely used in VOCs analyses (Allardyce et al., 2006; Smith and Španěl, 2011b, 2005b). It has well-defined analytical reaction conditions and the H_3O^+, NO^+ and $O_2^{+\bullet}$ reagent ions can be switched rapidly to analyse time-varying trace gases in air samples. In the present article, we report method development results aimed to selective analyses of individual monoterpenes in mixtures in air using a bespoke fast GC/SIFT-MS combination with H_3O^+ and NO^+ reagent ions. This involved the analysis of both prepared laboratory monoterpene/air mixtures and headspace of the foliage of different pine trees.
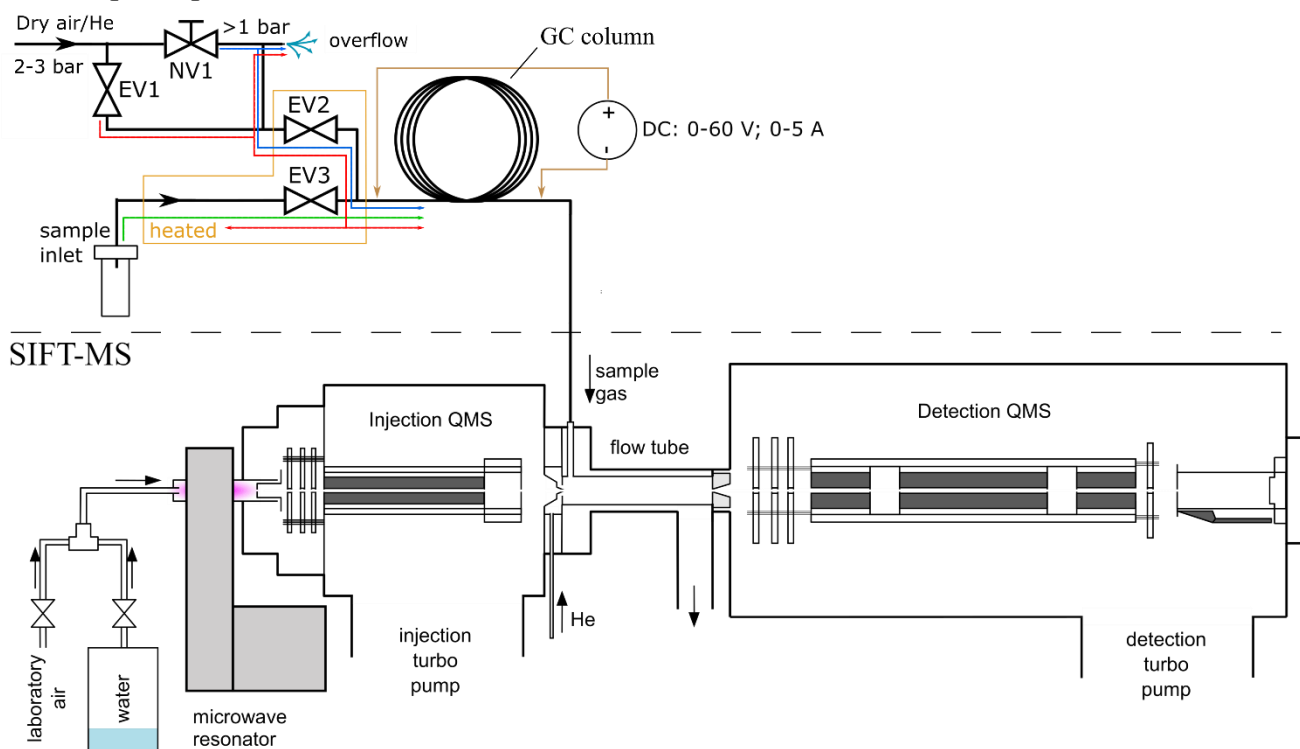
Figure 1: Schematic visualization of the fast GC-SIFT-MS experiment. Coloured dashed lines in the inlet part of the fast CG represent gas flow through the system of the valves EV1-3. The blue line traces the "normal mode" regime, the green line represents the "sampling mode" and the red line represents the "cleaning mode".

2 Construction of a fast GC device for pre-separation

The experimental setup of the bespoke fast GC setup constructed as an addition to SIFT-MS is shown in Fig. 1. The routing of the sample and the carrier gases was controlled by solenoid valves (Parker VSONC-2S25-VD-F, < 30ms response), labelled in Fig. 1 as EV1, EV2 and EV3. The needle valve NV1 was used in combination with an overflow relieve tube to fine-adjust the flow rate of the carrier gas (20-50 sccm from a gas cylinder regulator set to about 2 bar) so that the air pressure at the

column entrance is held just above ambient. The region of the sampling input line, EV2, EV3 and their connection with the column are permanently heated to ~60 °C to prevent adsorption of sample gas/vapour and to reduce memory effects.

Three modes of gas flow are possible as illustrated in **Fig. 1**:

- The **"normal mode":** EV2 is open and both EV1 and EV3 are closed. Carrier gas flows through NV1, partly vented via the overflow relieve but mostly into the column. The pressure at the column entrance is just above the ambient atmosphere and a constant flow rate of clean carrier gas (synthetic air or helium) is thus achieved.

- The **"sampling mode":** EV1 and EV2 are closed and EV3 is open. Sample air is introduced into the column in a short time (1 to 8 s) after which the "normal mode" is resumed.

- The **"cleaning mode":** All valves are open and the carrier gas taken directly from the cylinder regulator is introduced into the column (higher than normal flow) and purges the sample line via EV3. The overflow relieve flow rate is not sufficient to diminish the pressure.

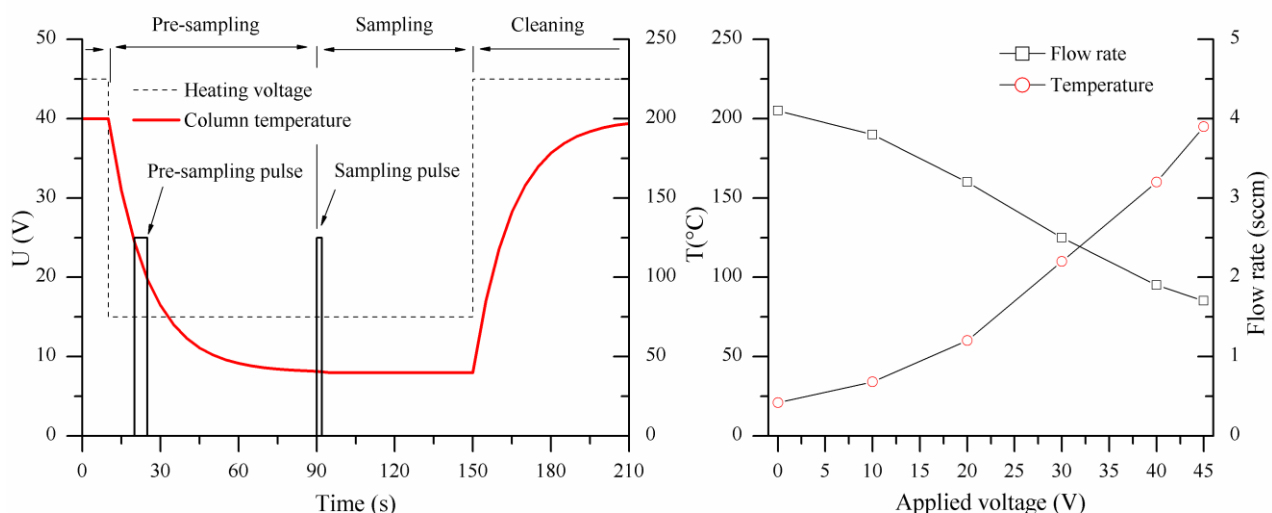The modes can be switched either manually or controlled from the SIFT-MS software.

Figure 2: Left: the applied heating voltage (dashed) and the temperature profile of the column (red) during the fast GC cycle. The pulses indicate the opening of the valve EV3 during the pre-sampling and the sampling periods. Right: The increase of the column temperature and the related decrease of the carrier gas flow rate with the heating voltage.

The operation sequence for air analysis is as follows: A column is first heated up to 200 °C in the "cleaning mode" for three minutes prior to commencing the "normal mode" with an appropriate heating voltage setting (e.g. 15 V as shown in Fig. 2). Whilst the column cools down, a pre-sampling interval (8-10 s "sampling mode", see Fig. 2) is applied in order to refill the "dead volume" comprising the EV3 valve and the sampling inlet by air at its entrance. After the column reaches working temperature and a steady flow of clean carrier gas is established, the sample for actual analysis is introduced by enabling the "sampling mode" for selected amount of time.

In the experiments, two different GC columns were tested. First, a 5 m long nonpolar general-purpose chromatography metallic column MXT-1 (0.28 mm × 0.1 um active phase, Restek Inc.) using dry air as the carrier gas, which was chosen according to the previous PTR-MS fastGC analyses (Romano et al., 2014). Additionally, a second, application-specific column for volatile organic pollutants, MXT-Volatiles (0.28 mm × 1.25 um active phase, Restek Inc.), was used with helium carrier gas. In order to facilitate direct resistive heating, the coil-shaped stainless steel columns (resistivity ~4.2 Ω/m) were electrically isolated and connected to a regulated 60 V, 5 A DC power supply. Appearance of cold spots was suppressed by ensuring that the electrical current runs through the entire length of the columns. The temperatures of the columns were monitored by a K-type probe connected to their centres (see the right part of Figure 2 for the temperature variation with applied voltage). It is interesting to note that the flow of sampled air established by the pressure difference between ambient atmosphere and the low pressure of the SIFT-MS flow tube changes with the column temperature due to the variation of the dynamic viscosity of the air (see Fig. 2). This effect can to be estimated and have to be included to a quantification calculation.

In the initial tests with the first generic MXT-1 column, the "sampling mode" duration was fixed at 1.8 s due to SIFT-MS software limitations. For the later tests with the second MXT-Volatiles column, the SIFT-MS operational software was upgraded to provide an arbitrary timing of the "sampling mode" duration, where we used 6 or 12 s sampling intervals. Sampling was repeated several times to improve signal quality. The GC separation then takes place over typically 60 – 300 s whilst the eluent is continuously analysed by SIFT-MS. It is possible to apply a heating ramp during this period.

Several heating ramp profiles were tested (see data for MXT-1 column in Fig. S1 in the Supplement); however, due to the short GC column and relatively long injection time, the monoterpene chromatogram peaks coalesced when the column temperature exceeded 60 °C and it was found that optimal chromatograms were obtained isothermally at 40 °C (15 V heating voltage). Effects of the heating voltage on the retention time and the chromatogram profile is illustrated in Fig. S4 in the Supplement (data for MXT-Volatiles column).

3 SIFT-MS analyses of the eluent

In the present study, the *Profile 3* SIFT-MS instrument (Instrument Science, Crewe, UK) was used (Smith et al., 1999). Reagent ions are formed in a microwave discharge through a mixture of water vapour and atmospheric air (see Fig. 1). A mixture of ions is extracted from the discharge and focused into a quadrupole mass filter where they can be analysed according to their mass-to-charge ratio, *m/z*. Thus, the reagent ions H_3O^+, NO^+ or $O_2^{+\bullet}$ can be selected ($O_2^{+\bullet}$ was not used in the present experiment) and separately injected into flowing helium carrier gas (pressure p = 1.4 mbar, temperature T = 24 °C). Any internal energy possessed by the reagent ions is rapidly quenched in collisions with helium atoms leaving a thermalized ion swarm that is convected down the flow tube. Sample gas is introduced into the helium/thermalized swarm at a known flow rate that changes with the GC column temperature. The reagent ions react with the VOC molecules in the sample gas during a time period defined by the known flow speed of the ion swarm and the length of the flow tube. At the end of the flow tube, the ionic products (analyte ions) generated by ion-molecule reactions are sampled by a pinhole orifice into the analytical

quadrupole mass spectrometer. The count rates of the reagent and analyte ions are obtained using a single channel electron multiplier. Thus, full scan (FS) spectra can be obtained over a chosen m/z range to identify the analyte ions or rapidly switched between selected m/z values using the multiple-ion monitoring mode (MIM) (Španěl and Smith, 2013; Smith and Španěl, 2011a). For the monoterpene study, FS mode was used for SIFT-MS analyses, whilst the MIM mode was used for fast GC-SIFT-MS setup. Typical count rate the reagent ions is one million cps, while amount of other ion lays below 1. Switching between two reagent ions requires milliseconds of time, as it depends mainly on the velocity of the carrier gas (12 000 cm.s^{-1}) and the length of the flow tube (5 cm). Therefore, the only limiting factor is a software sampling frequency, which depends on the amount of monitored ions, and is usually below one second.

3.1 Reactions of the H_3O^+ and NO^+ reagent ions with monoterpenes

In the present study, SIFT-MS analyses of monoterpenes were carried out using the previously investigated reactions of monoterpenes with H_3O^+ and $NO^{+\cdot}$ ions (Schoon et al., 2003; Wang et al., 2003). The H_3O^+ reactions are known to proceed via proton transfer forming $C_{10}H_{17}^+$ (m/z 137) that partially fragments to $C_6H_9^+$ (m/z 81) due to elimination of a C_4H_8 moiety from the nascent $(C_{10}H_{17})^*$ excited ion:

$$H_3O^+ + C_{10}H_{16} \rightarrow C_{10}H_{17}^+ + H_2O \tag{1a}$$
$$\rightarrow C_6H_9^+ + C_4H_8 + H_2O \tag{1b}$$

NO^+ reacts with monoterpenes by charge transfer forming the parent cation $C_{10}H_{16}^{+\cdot}$ (m/z 136) and a number of fragment ions, including $C_7H_9^+$:

$$NO^+ + C_{10}H_{16} \rightarrow C_{10}H_{16}^+ + NO \tag{2a}$$
$$\rightarrow C_7H_9^+ + NOC_3H_7 \tag{2b}$$

The exothermicity of charge transfer (2a) is represented by the difference between the ionization energies of the neutral NO (9.26 eV) and of the particular monoterpene (ranging from 8.07 eV for α-pinene to 8.4 eV for limonene) (Garcia et al., 2003; NIST). Other fragments, including $C_7H_8^+$, $C_7H_{10}^+$, $C_9H_{13}^+$ and $C_{10}H_{15}^+$, are also formed and the branching ratios between the channels (2a) to (2b) and other fragments depend on the isomeric structure of the monoterpene (Schoon et al., 2003; Wang et al., 2003) and are given in Table S1 in the Supplement. Based on this known ion chemistry, for the present study it was decided to analyse monoterpenes using both the H_3O^+ reagent ions by recording the $C_{10}H_{17}^+$ (m/z 137) and $C_6H_9^+$ (m/z 81) analyte ions and the NO^+ reagent ion by using the $C_{10}H_{16}^+$ (m/z 136) and $C_7H_9^+$ (m/z 93) analyte ions. To facilitate the identification of monoterpenes on the basis of the branching ratios of reactions (1) and (2), the product ion signal ratios [m/z 81]/[m/z 137] and [m/z 93]/[m/z 136] were determined under the conditions of the *Profile 3* SIFT-MS instrument using standard monoterpene mixtures, and these ratios (r) are given in Table 2, and discussed in Section 4.2.

The interaction of the primary ions with monoterpenes may be affected by presence of neutral water molecules and thus by different humidity of the sample. This was reported by Wang et al. (Wang et al., 2003) when decreased fragmentation of monoterpene product ions was observed in humid air samples, what result in decrease of our product ion signal ratio r (see Section 3.2). For H_3O^+ regent ions, this change was significant for β-pinene (r reducing from 0.75 to 0.51), R-Limonene (r

from 0.45 to 0.34) or 3-carene (r from 0.33 to 0.23). For the NO^+ reagent ion, a significant effect was observed only for α-pinene (r from 0.32 to 0.08) and β-pinene (r from 0.25 to 0.05).

3.2 Analysis of the product ion intensity ratios

To facilitate assignment of the fast GC elution peaks to specific monoterpenes, mean fragment ion fractions $r_i = f_i/g_i =$ [m/z 81]/[m/z 137] (or for NO^+, $r_i = f_i/g_i =$ [m/z 93]/[m/z 136]) were calculated for each interval of retention times t_1 to t_2, as the weighted mean of the product ion signal ratios $\overline{r_w}$:

$$\overline{r_w} = \sum_{i=t_1}^{t_2} w_i \frac{f_i}{g_i}; \ w_i = \frac{f_i + g_i}{\sum_{i=t_1}^{t_2} f_i + g_i}, \tag{3}$$

The weights (w_i) applied to each of several discreet measurements were based on the total signal of both ions f_i and g_i in order to emphasise the area within the peak. Time intervals t_1 to t_2 were chosen for each isomer as the area of the chromatographic peak where the total ion signal was >10% of the peak value.

The quality of the ratio estimation was assessed from the variation of the f_i/g_i ratio estimated as

$$\sigma_i^2 = Var(f/g) \approx \frac{\mu_f^2}{\mu_g^2}\left(\frac{\sigma_f^2}{\mu_f^2} + \frac{\sigma_g^2}{\mu_g^2}\right) = \frac{\mu_f^2}{\mu_g^2}\left(\frac{\lambda_f + \sigma_{bg_f}^2}{\mu_f^2} + \frac{\lambda_g + \sigma_{bg_g}^2}{\mu_g^2}\right), \tag{4}$$

where μ_f and μ_g represent intensities of the selected fragments and σ_f^2 and σ_g^2 are the variances of the μ_f and μ_g intensities estimated according to the Poisson distribution as the sum of distribution variance equal to the expected value $\lambda = \mu$ and background variance σ_{bg}^2 (Van Kempen and Van Vliet, 2000).

From this variation, the standard error of the weighted mean was calculated as:

$$\sigma_{\overline{r_w}} = \sqrt{\sum_{i=t_1}^{t_2} w_i^2 \sigma_i^2} \tag{5}$$

The weighted standard deviation of the f_i/g_i ratios was also routinely calculated as:

$$s = \sqrt{\frac{\sum_{i=t_1}^{t_2} w_i\left(\frac{f_i}{g_i} - \overline{r_w}\right)^2}{1 - \sum_{i=t_1}^{t_2} w_i^2}} \tag{6}$$

3.3 Fast GC SIFT-MS quantification

The total amount of eluting analyte, C, in each GC peak is determined by SIFT-MS from the area under the curve from the number density of the analyte molecules [M] (Španěl et al., 2006) in the flow tube recorded as a function of time, t, according to the equation:

$$C = \frac{1}{N_A} \int_0^{t_{max}} [M] S \, dt, \tag{7}$$

where N_A is the Avogadro constant and S is the constant volume flow rate of the sample and carrier gas mixture flowing into the SIFT-MS carrier gas as determined by the pumping speed of the SIFT-MS primary vacuum pump. Note that the flow rate of GC eluent gas does not enter this calculation and does not directly affect the determined amount of analyte expressed in

nanomoles, nmol. [M] is calculated by the *Profile 3* software according to the SIFT-MS general method for the calculation of absolute trace gas concentrations from the reagent and product ion count rates, the reaction rate constants (see Table S1 in the Supplement) and the reaction time considering differential diffusion losses (see equation 15 in reference (Španěl et al., 2006). The amount of analyte is proportional to its concertation [A] in sampled air and the sampled volume, *V*, given by the sampling flow rate (usually 3 sccm) and time (1.8 to 12 s) as:

$$C = [A]\frac{V}{V_m},$$
(8)

where $[V_m] = 24.0$ L/mol is the molar volume of air at 293 K.

3.4 Reference chemicals and plant samples

All monoterpenes used in the experiments, viz. ((+)-α-pinene (98%), (+)-β-pinene (≥98.5% analytical standard), camphene (95%), myrcene (≥90% analytical standard), 3-carene (≥98.5% analytical standard), R-limonene (≥99.0% analytical standard), α-terpinene (≥95%) and γ-terpinene (97 %), were purchased from Sigma-Aldrich Co. Individual monoterpene vapour standards and monoterpene vapour mixtures were prepared by the diffusion tube method (Thompson and Perry, 2009). Thus, for individual standards, about 5 µl of each monoterpene was placed in a 2 ml vial closed by PTFE septum caps. Each vial was then penetrated with a diffusion tube (1/16" OD x 0.25 mm ID x 5 cm length PEEK capillary) and placed into a 15 ml glass vial closed by a PTFE septum. The headspace of the 15 ml vial was sampled after stabilization (>30 minutes) of the concentration. Humidity of the headspace was typically 1.5% water vapour by volume as determined by SIFT-MS. For the α-pinene, the intensities were too high and thus they had to be reduced by placing only trace amount of sample into the 2ml vial. For the mixture preparations, a similar approach was used; several vials containing different monoterpene, penetrated by PEEK capillaries, were placed together into a 500 ml bottle. Note that the concentrations of the individual isomers in the mixture are different due to the variations in their saturated vapour pressures. The same mixture was used for H_3O^+ and NO^+ experiments with the MXT-1 column.

To demonstrate the applicability of the fast GC/SIFT-MS analyses to real samples, three different types of coniferous tree needles were prepared: Spruce (*Pincea punges*), Fir (*Abies concolor*) and Pine (*Pinus nigra*) (see Fig. S5 – S7 in the Supplement). For the first study using the MXT-1 column, the needle samples (0.26 g Spruce, 0.42 g Fir and 0.32 g Pine) were collected in the urban area of Prague in June 2017 and stored in 10 ml vials from which the headspace was sampled 30 min after harvesting. For the later study using the MXT-Volatiles column, pine tree twigs were collected in June 2018 from the same trees (21.8 g Spruce, 21.4 g Fir and 20.6 g Pine). The exposed cuts of the twigs were sealed by wrapping the parafilm around the cut. The samples were placed into a Nalophan bag of volume approximately one litre. During the analyses, the laboratory was thermalized to the outdoor temperature (about 30 °C) to reduce thermal shock to the samples. In the laboratory, only a scattered natural light was present.

4 Results and discussion

To investigate if the various monoterpenes in a mixture could be effectively distinguished using SIFT-MS enhanced by the fast GC pre-separation, eight common biogenic monoterpenes were investigated. Individual monoterpene standards were analysed first with both MXT-1 and MXT-Volatiles column to obtain the instrument response in terms of retention times and product ion ratios using two reagent ions H_3O^+ and NO^+. The separation of monoterpenes was demonstrated through analysis of prepared monoterpene mixture. Separation of both GC columns was compared using isothermal GC at temperature 40 to 45 °C. The elution times of all studied monoterpenes were within 45 s of total retention time for MXT-1 column and within 180 s for MXT-Volatiles column. Using the information on the ratios of ion products for the H_3O^+ and NO^+ reactions together with the GC retention times, it was possible to identify the composition of a reference standard mixture. Finally, the same procedure was used to analyse the leaf headspace of three coniferous samples to demonstrate the analysis of real samples.

4.1 Comparison of columns: MXT-1 vs. MXT-Volatiles

In the present experiment we used heated columns isothermally to the temperature app. 40 °C due to the behaviour of the MXT-1 column. For higher temperatures, the monoterpene chromatogram peaks coalesced while for lower temperatures a significant influence of the lab air temperature fluctuations was apparent. At these conditions for MXT-1 column, monoterpenes are not fully separated and thus, fast GC with MXT-1 column alone (at 40 °C) provides only qualitative analysis. The retention times determined from the chromatograms obtained for individual monoterpenes at 40 °C are given in Table 2. For MXT-1 column, the apparent difference in retention times observed between the two reagent ions was probably caused by the temperature fluctuations of the column. Whilst the retention times for individual monoterpenes are different, they are not sufficiently stable (fluctuate by > 1 s, see Table 2) in the present fast GC device for analyses based on retention time only to be reliable. A noticeable effect of ambient temperature on the rate of passive column cooling was observed resulting in changes of the column temperature profile and thus in variations of the monoterpene retention times. Therefore, for longer column and higher temperature it may be reduced. Use of the MXT-Volatiles column resulted in about five times longer retention times and better GC peaks separation at the same operational conditions (flow rate, temperature and pressure) due to the higher efficiency of the 1.25 um active phase (compared to 0.1 um for MXT-1 column).

The quality of the separation could be increased by using hydrogen as a carrier gas and by a faster sample injection, as demonstrated by Materic et al. (Materić et al., 2015) with fastGC PTR-MS by where complete separation of monoterpenes was achieved using the MXT-1 column. As observed for both columns, separation can be improved by decreasing the column temperature (see Fig. 3 and Fig. S4 in the Supplement), however this increase the chromatogram width.

Table 2: Ratios of the H_3O^+ and NO^+ reaction product ion signals and the GC retention times, s, for the eight monoterpenes at columns temperature 40 °C. Also given are the saturated vapour pressures in Torr. The standard error of the fast GC $\overline{r_w}$ values for individual monoterpenes estimated by Eq. (5) is less than 5% (except 8.6% for camphene), overall less then ±0.02.

Compound	[*m/z* 81]/[*m/z* 137]		[*m/z* 93]/[*m/z* 136]		Retention time [s]		
	H_3O^+		NO^+		H_3O^+	NO^+	H_3O^+
Saturated vapour pressure (Torr)	Literature Schoon [a] Wang [b]	Results *Full scan fast GC MIM*	Literature Schoon [a] Wang [b]	Results *Full scan fast GC MIM*	MXT-1	MXT-1	MXT-Vol
α-pinene	0.45	0.67[c]	0.05	0.16[c]	16	14.7	72
4.75[e]	0.64	0.46[d]	0.09	0.19[d]			
camphene	0.1	0.14[c]	0	-	17	17.7	83
2.50[e]	0.16	0.16[d]	0.01	0.03[d]			
β-pinene	0.52	0.61[c]	0.03	0.12[c]	20.4	22	106
2.93[e]	0.67	0.66[d]	0.08	0.17[d]			
myrcene	0.44	0.72[c]	0.36	0.72[c]	18.5	17.8	134
2.09[f]	0.52	0.51[d]	0.62	0.63[d]			
3-carene	0.24	0.39[c]	0.05	0.12[c]	25.5	25.6	142
3.72[h]	0.32	0.35[d]	0.1	0.15[d]			
α-terpinene	-	0.14[c]	-	0.01[c]	27	25.1	157
1.64[h], 1.66[i]	0.11	0.17[d]		0.01[d]			
R-limonene	0.30	0.43[c]	0	0.03[c]	27.5	31	170
1.98[g]	0.43	0.41[d]	0.01	0.06[d]			
γ-terpinene	-	0.18[c]	0.08	0.08[c]	40.4	32.5	184
1.07[h], 0.7[j]	0.21	0.16[d]	0.09	0.09[d]			

[a] (Schoon et al., 2003); [b] (Wang et al., 2003); [c] Present result based on SIFT-MS measurement; [d] Present result based on fast GC-SIFT-MS measurement; saturated vapour pressures in Torr at 25 °C are according to [e] (Daubert, 1989), [f] (Haynes, 2014), [g] (Yaws, 1994), [h] (TGSC), [i] (Takasago, 2011), and at 20 °C according to [j] (ChemicalBook, 2016).
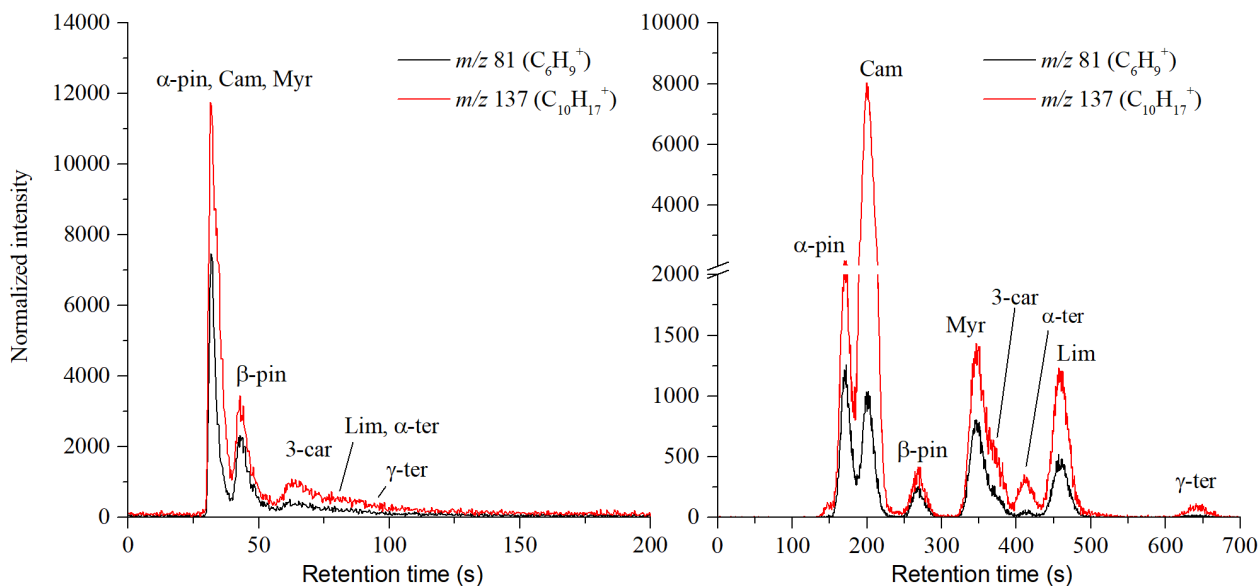
Figure 3: Chromatograms of mixture of monoterpenes at room temperature obtained using MXT-1 column (left) and MXT-Volatiles column (right). Chromatogram peaks in the MXT-1 column are not fully separated, but separation takes below 150 s compare to 700 s required for MXT-Volatiles column. The signal intensities are the analyte ion count rates normalized to the H_3O^+ reagent ion count rate of 10^6 s^{-1}.

The performance of both MXT-1 and MXT-Volatiles columns were compared by analyses of a gas mixture of eight monoterpenes. For the MXT-1 column, four characteristic GC peaks were identified for both reagent ions, marked as A, B, C and D with retention time of 17.6 s, 20.8 s, 26.3 s and ~30 s for H_3O^+, and 17.5 s, 20.7 s, 26.3 s and ~30 s for NO^+ (see Fig. 4). Based on the retention times obtained for individual monoterpenes (see Table 2 and Fig. S2 in the Supplement), peak A is due to co-elution of α-pinene, camphene and myrcene. Peak B is due to the presence of β-pinene exclusively and peaks C and D are due to the remaining four monoterpenes, mainly 3-carene and R-Limonen. Note that the individual peak heights are influenced by the monoterpene saturated vapour pressures (see Table 2). Using the MXT-1 column at these conditions it is not possible to achieve separate GC peaks for individual monoterpenes, however qualitative analysis is possible.

The MXT-Volatiles column facilitates identification of all monoterpenes present in the mixture for temperatures close to the room temperature (see Fig. 3). For the MXT-Volatiles tests, the sampling mode was extended to 12 s, representing the collection of approximately 0.6 mL of the monoterpene mixture headspace. At column temperature 40 °C, the monoterpene peaks are well separated, however, α-pinene and camphene are likely to co-elute as they are usually very intensive. It is interesting to note that the chromatogram (see Fig. S4 in the Supplement) changes with the temperature of the column and additional peaks appear at higher temperatures probably as a result of presence of different conformers. It thus seems that at the column temperature ~45 °C using 20 V heating voltage (see Fig. 4) in the mixture chromatogram the small β-pinene is hidden behind the second camphene peak and the α-terpinene peak also disappears (see also the fragmentation analyses later in section 4.2).
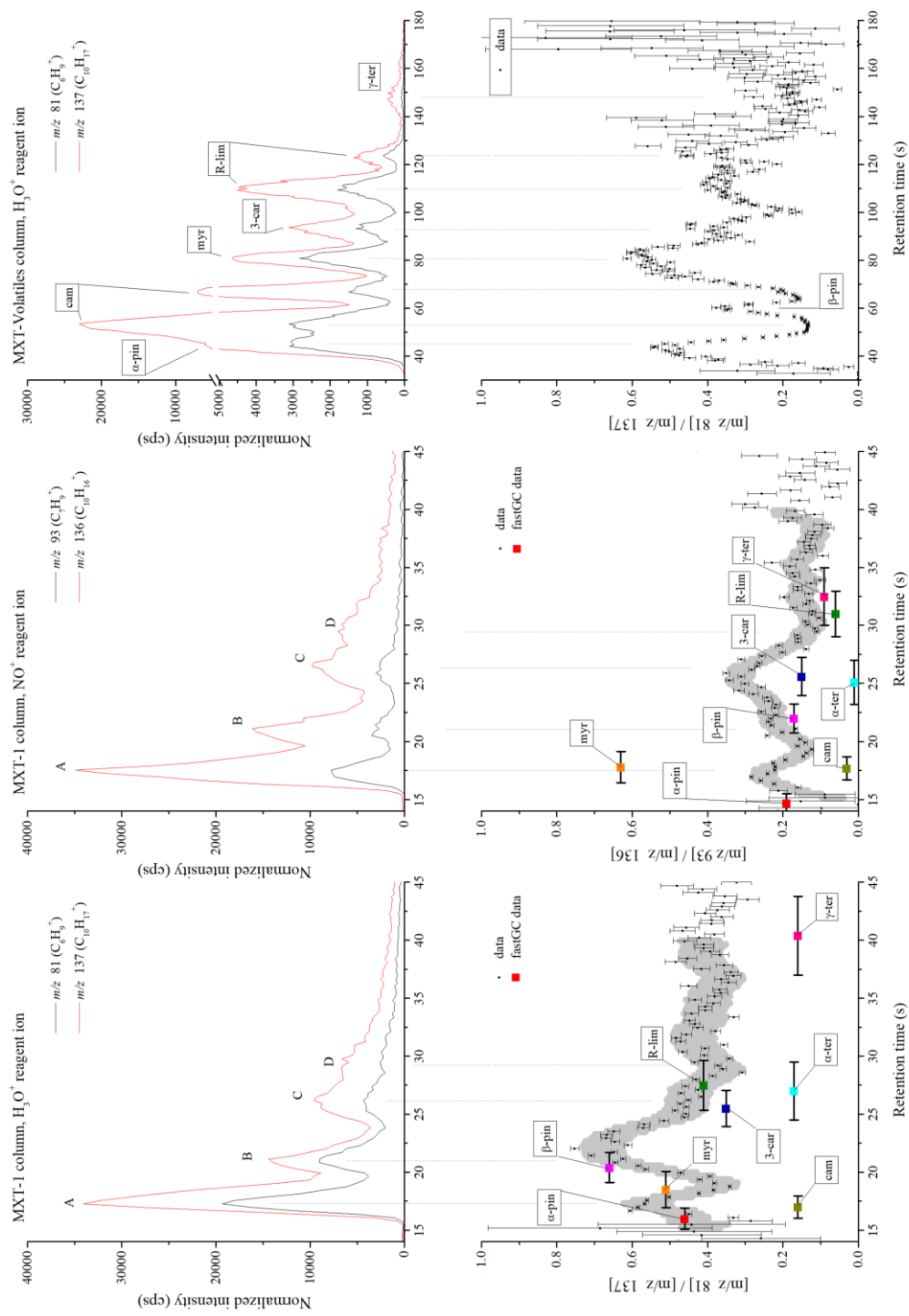
Figure 4: Chromatograms of the mixture of monoterpenes (upper figures) measured by H3O$^+$ (left) and NO$^+$ (right) reagent ions, obtained using the MXT-1 column. A, B, C, D represent characteristic peaks in the chromatogram. For each chromatogram, the product ion signal ratio r; is presented in the lower figures. The grey data background represents the calculated standard deviation of the data by Savizky-Golay smoothing between 15 s and 40 s. The position and value of the ratio for individual monoterpenes is based on the fast GC MXT-1 measurements presented in Table 1. Note that the retention times are determined by the fast GC conditions and do not depend on which SIFT-MS reagent ion is used. The signal intensities are the analyte ion count rates normalized to a reagent ion count rate of 10^6 s^{-1}.

13

4.2 Analysis of product ratio and use of the NO⁺ reagent ions

The inadequate separation of monoterpenes due to a short column or high temperature (as the case of MXT-1 column) can be mitigated by the analysis of the product ion signal ratios r_i (see Sec. 3.2) and additionally by using an additional reagent ion. It may be possible to improve identification of myrcene or camphene (often co-eluted with a-pinene) as well as of other monoterpenes by exploiting different ion chemistry of the NO⁺ regent ions. These data in combination with H_3O^+ data allow identification of compounds on the basis of the ratios of in total four different product ions. Use of NO⁺ regent ions was applied only on MXT-1 column, as full separation of monoterpenes using H_3O^+ reagent ions was not achieved and thus retention time cannot be effectively used as parameter for their identification. Hoverer, as will be presented, use of the NO⁺ regent ions brings additional benefits and thus it may be a valuable source of information even for fully separated chromatograms. Note that the retention times are determined by the fast GC conditions and do not depend on which SIFT-MS reagent ion is used (see Table 2).

The $\bar{r_w}$ values (see Table 2) obtained from the SIFT-MS FS data and the MIM data for the fast GC peaks for most of the isomers are in good agreement. However, the ratios obtained for α-pinene and myrcene are somewhat variable between the FS and MIM data and they also differ somewhat from the literature values (α-pinene from 0.45 to 0.67 for H_3O^+, myrcene from 0.44 to 0.72 for H_3O^+). This may be caused by different humidities of the samples, as discussed in Section 3.1., where it was seen that increase of humidity lower the $\bar{r_w}$ values. In fast-GC setup, water retention time is much lower as the retention time for monoterpenes, thus water influence on ion chemistry is for most monoterpenes negligible. Slightly affected can be α-pinene as he is the first one presented in the chromatogram. Therefore, only $\bar{r_w}$ values obtained using the fast CG will be used for further study. The standard error of the fast GC $\bar{r_w}$ values for individual monoterpenes estimated by Eq. (5) (using the MXT-1 column) is less than 5% (except 8.6% for camphene) and is smaller than the observed variability between the methods. The $\bar{r_w}$ values for MXT-Volatiles column were similar to those obtained with MXT-1 column, as expected.

Analysis of $\bar{r_w}$ values can be now used to improve identification of monoterpenes in measured mixtures. For MXT-1 column, the $\bar{r_w}$ values for peaks A, B, C and D were calculated as 0.49, 0.63, 0.45, 0.40 respectively for H_3O^+ and as 0.21, 0.21, 0.27, 0.14 for NO⁺. Based on these ratios (using fast GC data from Table 2), peak B could clearly be assigned as β-pinene. However, the remaining peaks contain several isomers and thus the $\bar{r_w}$ values are not providing unique identifications. So dynamic variations of r_i needed to be investigated to see if they can provide additional information. The time profile r_w in chromatogram is shown in the bottom part of Fig. 4. To recognize trends in these data, Savizky-Golay smoothing (Savitzky and Golay, 1964) was used (second polynomial order across 10 data points, OriginPro 9.0 (OriginPro, 2018). Also plotted (grey area in Fig. 4) is the standard deviation of the data points from the smoothed line in the interval of retention times from 15 s to 40 s. Note that this standard deviation is greater than the standard error of the data points, possibly due to a lower accuracy of data at the longer retention times. The standard deviation allows assessment of the significance of the changes in $r_i = f_i / g_i$.

According to the elution time, the first chromatographic peak A consist of three monoterpenes: α-pinene, camphene and myrcene. For the H_3O^+ reagent ions, the $\overline{r_w}$ value corresponds to both α-pinene and myrcene considering the $\overline{r_w}$ value for peak A (0.49) or r_w close to the peak maxima (0.55–0.6). However, a more obvious difference between α-pinene and myrcene is observed using the NO^+ reagent ions. The value of the weighted mean ratio for the peak A (0.21) is close to the ratio for α-pinene. In the maxima of peak A, however, r_w approaches the value of 0.3, which is close to the value expected for a combination of both these monoterpenes (0.32, considering the data from fast GC measurement and the vapour pressure in Table 2). For camphene, r_w in the chromatograph did not reach the low values expected for both reagent ions. However, its presence is clearly visible as a dip in r_w situated between the peaks A and B. In the absence of camphene, the ratio should linearly move to values characteristic for the peak B without any dip. The depth of the dip does not reach the ratio value expected for camphene due to a persistent tails of the peaks for both α-pinene and myrcene.

Peak B in the chromatograms is identified as β-pinene by its retention time. The $\overline{r_w}$ values for the H_3O^+ and NO^+ reagent ions are 0.63 and 0.21, respectively. The values r_w are similar to $\overline{r_w}$ and slightly higher than to the fast GC standard values for β-pinene (see Table 2).

Peaks C and D are not clearly separated in the chromatogram. For the H_3O^+ reagent ions, the $\overline{r_w}$ value is similar for both peaks; thus, the presence of limonene, 3-carene or α-terpenine is likely since the $\overline{r_w}$ values for the peaks C (0.45) and D (0.4) are comparable with the analyte signal ratios (see Table 2) for limonene and 3-carene. A lower r_i for α-terpinene might be observed as a dip similar to camphene. However, the observed dip in r_i at the D peak is not so statistically significant as the dip for camphene, and the vapour pressure for both α- and γ-terpinene are lower than other monoterpenes. Analysis of the C and D peaks using the NO^+ reagent ion shows a clearer difference between them. The calculated $\overline{r_w}$ for the peak C (0.27) as well as the maximum r_i (0.35) are, unexpectedly, much higher than for the remaining monoterpenes. This can be explained only by the influence of myrcene or by the presence of impurities in the form of an additional monoterpene in the mixture (for example ocimeme has high r_i of 0.62 (Wang et al., 2003)). Amongst the eight monoterpenes, 3-carene has the highest r_i within the retention time of peak C. The second peak D (0.14) can be then associated with R-limonene, which has a low r_i (0.06) for NO^+ reagent ions, with some contribution by α-terpinene. The presence of γ-terpenine is not visible due to its low vapour pressure, but there may be some contribution in the D peak, but much smaller than the contribution by limonene.

To summarize, combining analyses using both H_3O^+ and NO^+ reagent ions with dynamic variations of r_i allows the identification of α-pinene, camphene and myrcene in peak A followed by the presence of β-pinene in peak B exclusively. Peak C is characterized as 3-carene and peak D as R-limonene and/or α-terpinene. γ-terpenine contributes only weakly due to its low vapour pressure and has no recognisable response in the chromatogram compared to the remaining monoterpenes.

Analysis of the $\overline{r_w}$ values for MXT-Volatiles column is more simple due to better separation of peaks. Value of r_i clearly change for different monoterpenes, according the expected $\overline{r_w}$ values for individual monoterpenes. Usefulness of the r_i analysis for MXT-Volatiles column can be observed in analysis of β-pinene, which is featureless compare to the camphene. Camphene, additionally, produce second chromatographic peak, which can be easily incorrectly associated with β-pinene.

Analysis of the r_i show values below 0.2 for both peak maxima, characteristic for camphene. Presence of β-pinene is visible as increase of r_i value up to 0.4 at retention time 60 s.

4.3 Tree samples investigation using the MXT-1 column

To test how fast GC-SIFT-MS is applicable for analyses of real biological samples, VOC emissions were analysed from three fresh coniferous tree needle samples: spruce, fir, and pine as shown in Fig. 5. MS obtained using the H_3O^+ regent ion are shown in Fig. S3 in Supplement. Based on the results of the above GC data for standard monoterpene mixtures, the chromatograms were divided into three areas. The first part characterized by the presence of α-pinene, camphene and myrcene between retention times of 12-18 s, the second part characterized by the presence of β-pinene with retention times between 18-25 s and the third part characterized by presence of 3-carene and limonene with retention times between 25-40 s. The $\overline{r_w}$ values were calculated for the selected regions as follows

- Spruce: The first region of the main peak 0.35 (H_3O^+), 0.11 (NO^+). Note that the very low $\overline{r_w}$ for NO^+ indicates the absence of Myrcene. The $\overline{r_w}$ value for H_3O^+ is lower than expected for β-pinene and higher than expected for camphene. Therefore, the first peak is formed mainly from α-pinene, perhaps with small amount of camphene. The second region of a small peak 0.38 (H_3O^+) and 0.14 (NO^+). $\overline{r_w}$ for H_3O^+ is lower than expected for β-pinene and higher than that for camphene, signal therefore belongs to the decay of α-pinene. The signal ratio 0.38 (H_3O^+), 0.14 (NO^+) in the third region indicates presence of R-limonene or 3-carene.

- Fir: The chromatogram shows two intense peaks. The calculations of $\overline{r_w}$ for the first region (0.40 for H_3O^+, 0.14 for NO^+) and for the second region (0.56 for H_3O^+, 0.15 for NO^+) indicate the presence of both α-pinene and β-pinene. The decreasing $\overline{r_w}$ for the H_3O^+ reagent ions in the last part (0.48 for H_3O^+, 0.19 for NO^+) indicates the presence of 3-carene .

- Pine: Chromatogram contains only one peak. $\overline{r_w}$ is stable for both reagent ions for all retention times (0.55 for H_3O^+, 0.21 for NO^+ for the first sector; 0.57 for H_3O^+, 0.22 for NO^+ for the second sector; 0.57 for H_3O^+, 0.22 for NO^+ for the third sector). Together with the retention time of the peak (16.4 s) this certainly corresponds to α-pinene.

Concentrations of individual monoterpenes were calculated according to the procedure described in Section 3.3 for all selected regions. Calculation of monoterpene concentrations depends primarily on the individual reaction rate constants (see Table S1 in Supplement), which change from 2.3 to 2.6 for H_3O^+ and from 2.0 to 2.3 for NO^+ (in units of $10^{-9}cm^3s^{-1}$). Incorrect identification of monoterpened will thus lead to maximum 20% error in the concentration calculation. According to the $\overline{r_w}$ values in selected regions, the most representative rate constant was adopted to calculated monoterpene concentration in the selected region (see Table 3).

Table 3: Calculated concentrations of monoterpenes (in ppm and %) in the headspace over coniferous needles in selected regions of chromatogram obtained using MXT-1 column at column temperature 40 °C, using injection time 1.8 s and column flow 3 sccm. Rate constant used for calculation of concentration in selected regions was chosen according to $\overline{r_w}$ analysis.

Sample	Concentration (ppm, %)			
	12-18s	18-25s	25-40s	Sum 12-40s
Spruce (H_3O^+)	11.0[A], **42%**	9.0[A], **35%**	5.2[R], 5.9[3], **23%**	25.2 [A,R], 25.9 [A,3]
Spruce (NO^+)	14.5[A], **50%**	6.6[A], **23%**	7.4[R], 7.7[3], **27%**	28.5 [A,R], 28.8 [A,3]
Fir (H_3O^+)	177[A], **32%**	274[B], **49%**	95[R], 107[3], **19%**	546 [A,B,R], 558 [A,B,3]
Fir (NO^+)	117[A], **31%**	191[B], **51%**	74[R], 77[3], **18%**	372 [A,B,R], 375 [A,B,3]
Pine (H_3O^+)	195[A], **55%**	112[A], **31%**	43[R], 49[3], **14%**	350 [A,R], 356 [A,3]
Pine (NO^+)	128[A], **48%**	100[A], **37%**	38[R], 41[3], **15%**	266 [A,R], 269 [A,3]

Calculations were performed using the reaction rate constants for [A] α-pinene, [B] β-pinene, [R] R-limonene or [3] 3-carene.
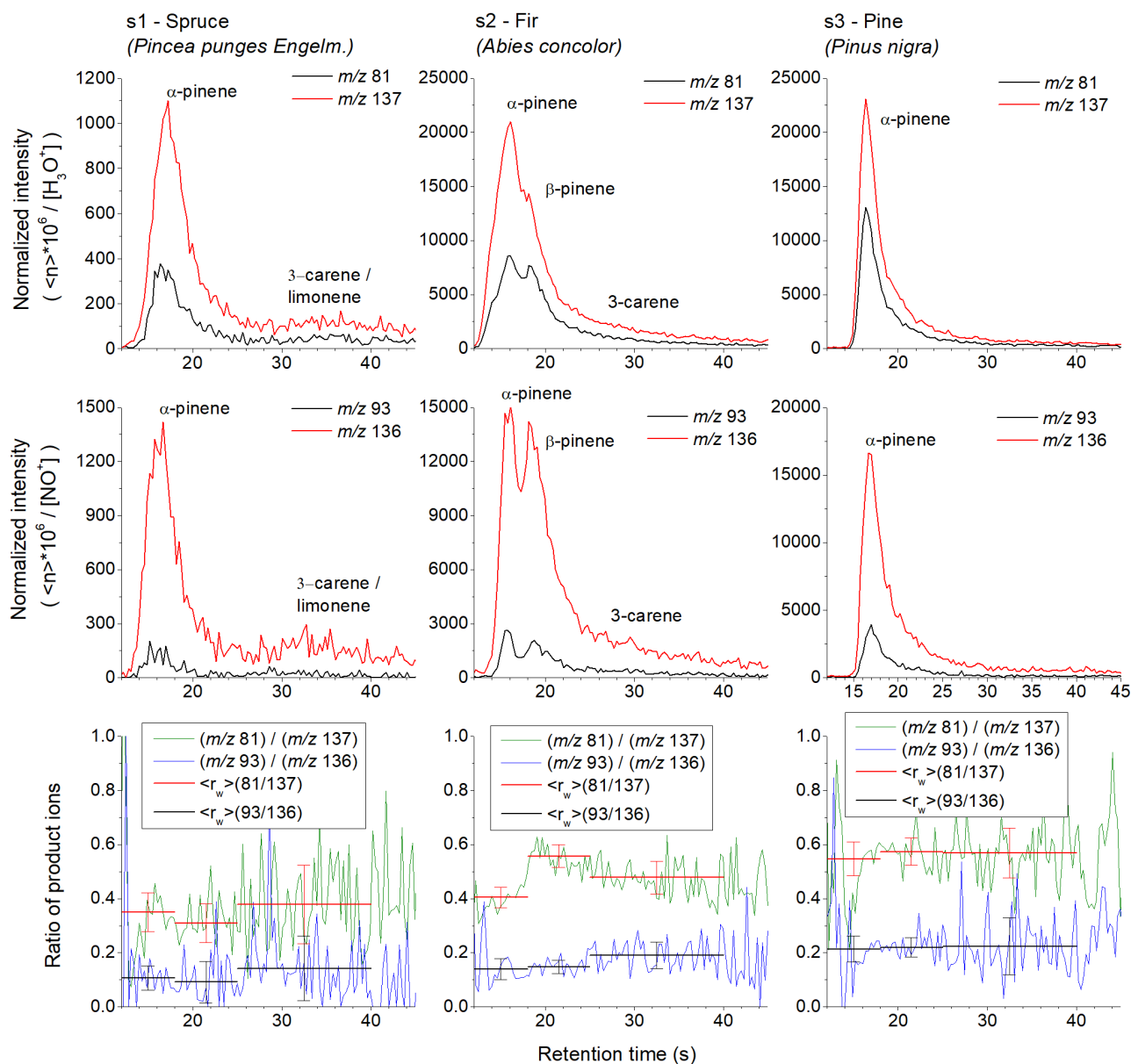
Figure 5: Chromatograms derived using the product ions for the reactions of H_3O^+ (upper row) and NO^+ (lower row) reagent ions with monoterpenes obtained for the three investigated pine tree samples (s1, s2 and s3) using the MXT-1 column. The signal intensities are the analyte ion count rates normalized to a reagent ion count rate of 10^6 s^{-1}. The black and red curves represent $C_6H_9^+$ (m/z 81) and $C_{10}H_{17}^+$ (m/z 137) product ions for H_3O^+ and $C_7H_9^+$ (m/z 93) and $C_{10}H_{16}^+$ (m/z 136) product ions for NO^+ reagent ions. The last row shows calculated ratios of product ions r_i for both reagent ions (green and blue curves) and for peaks areas calculated $\overline{r_w}$ (red and black).

4.4 Tree samples analyses using the MXT-Volatiles column

Similar experiments were conducted also using the MXT-Volatiles column, although on a different set of coniferous samples. The retention times for the individual monoterpenes were taken from the standard data obtained at the same column temperature (40 °C). The headspaces of the prepared tree needle samples were sampled for 6 s, representing a volume of 0.3 mL. The chromatograms obtained for the spruce, fir and pine samples are shown in Fig. 6 and represent the means of analyte ion count rates from 5 consecutive runs normalized to a constant reagent ion count rate of 10^6 s^{-1}.

- Spruce: In the chromatogram, four peaks were observed . The first peak with a retention time of 68 s corresponds to α-pinene with $\overline{r_w}$ of 0.60 for H_3O^+ and 0.24 for NO^+ regent ions. The tailing edge of the first peak shows a decrease of $\overline{r_w}$ (0.29 for H_3O^+, 0.14 for NO^+) due to a small contribution by camphene. The second peak corresponds to β-pinene, characterized by a retention time of 94 s with $\overline{r_w}$ of 1.05 for H_3O^+ and 0.50 for NO^+. The standard deviation in r_w was unfortunately substantial (±0.6 for H_3O^+, ±0.73 for NO^+). The position of the third peak corresponds to myrcene. The $\overline{r_w}$ values (0.43 for H_3O^+, 0.41 for NO^+) were again imprecise due to the low intensity and do not fully agree with the unique $\overline{r_w}$ for myrcene (see Table 2). The observed weak peak could therefore be due to other monoterpenes other than those eight included in Table 1. The last peak corresponds to 3-carene with $\overline{r_w}$ as 0.48 for H_3O^+ and 0.16 for NO^+ reagent ions

- Fir: In the chromatogram, three peaks are presentwhere the first is due to both α-pinene and camphene. Transition of $\overline{r_w}$ from the left (0.57 for H_3O^+, 0.23 for NO^+) to the right (0.22 for H_3O^+, 0.04 for NO^+) part of the first peak is clearly visible on the Fig. 6 in middle column. The first peak of the fir sample thus consists of two isomers. The second peak is due to β-pinene ($\overline{r_w}$ 0.80 for H_3O^+, 0.26 for NO^+) and the third peak by 3-carene ($\overline{r_w}$ 0.39 for H_3O^+, 0.15 for NO^+).

- Pine: Chromatogram shows three clear peaks of α-pinene (0.73 for H_3O^+, 0.30 for NO^+), β-pinene (0.92 for H_3O^+, 0.26 for NO^+) and 3-carene (0.49 for H_3O^+, 0.13 for NO^+) with just a very small and statistically insignificant indication of camphene. The retention times for α-pinene, β-pinene and 3-carene were 69.6 s, 97 s and 141 s, respectively.

Some differences can be seen between the results from the MXT-1 and MXT-Volatiles columns. The most significant difference is the presence of a camphene peak in the fir sample headspace, and the presence of β-pinene and 3-carene in the pine sample headspace when the MXT-Volatiles column was used. However, samples were collected at different times of the year and the character of the samples was also different (only needles for MXT-1 and whole twigs for the MXT-Volatiles analyses). Different sample sources could cause differences in monoterpene concentration as well (see Table 4).

Table 4: Calculated concentrations of monoterpenes (in ppm and %) in the headspace over coniferous twigs in selected regions of chromatogram obtained using MXT-Volatiles column at column temperature 40 °C, using injection time 6 s and column flow 3 sccm. Rate constant used for calculation of concentration in selected regions was chosen according to $\overline{r_w}$ analysis.

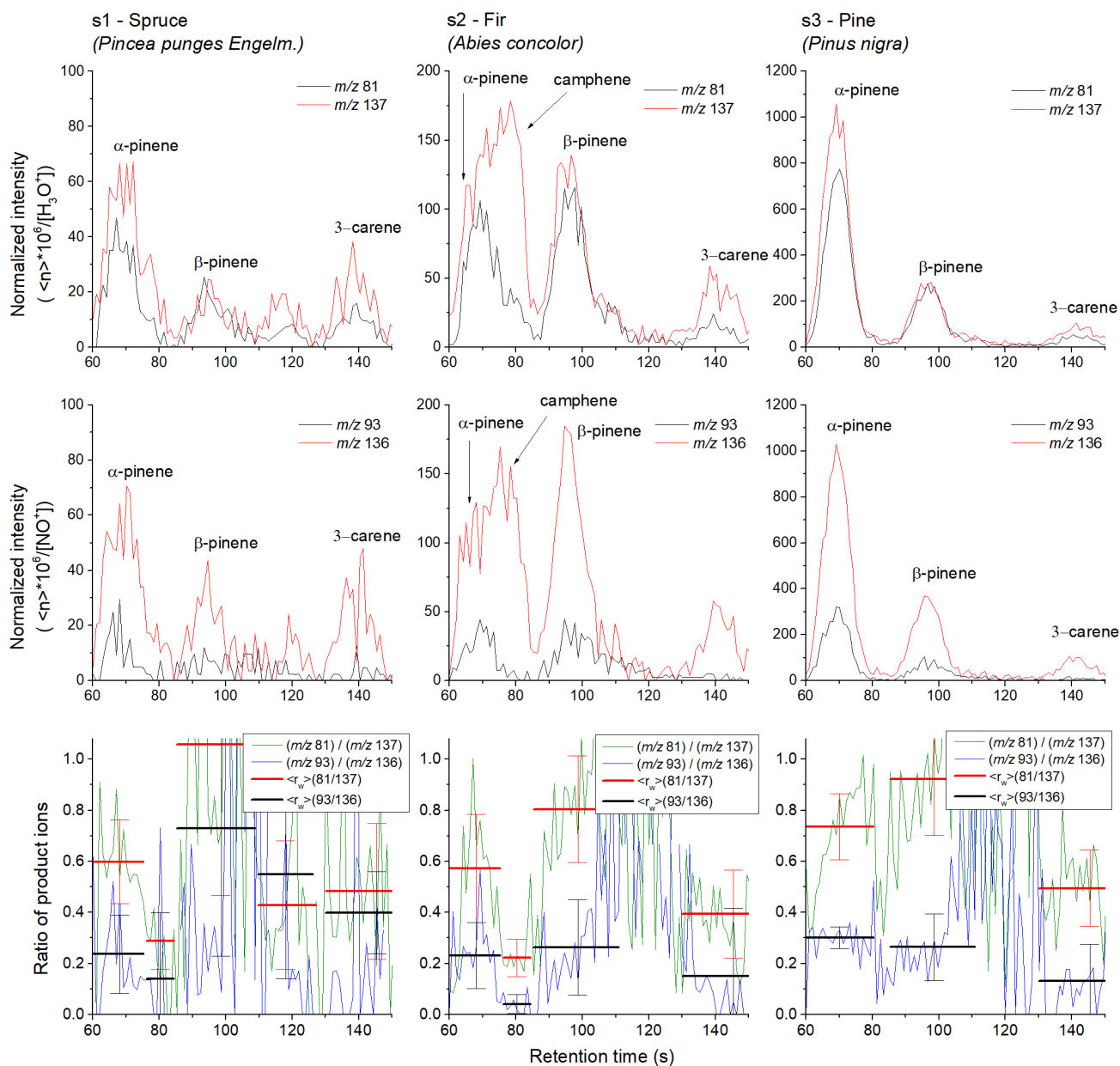| Sample	Concentration (ppm, %)				
	α-pinene	Camphene	β-pinene	3-carene	Sum5
Spruce (H_3O^+)	0.97, **46%**	0.21, **10%**	0.46, **22%**	0.48, **22%**	2.12
Spruce (NO^+)	0.74, **36%**	0.26, **13%**	0.56, **27%**	0.49, **24%**	2.05
Fir (H_3O^+)	2.51, **31%**	1.46, **18%**	2.9, **36%**	1.17, **15%**	8.04
Fir (NO^+)	1.97, **28%**	1.29, **19%**	2.80, **40%**	0.88, **13%**	6.94
Pine (H_3O^+)	15.5, **65%**	nd	5.95, **25%**	2.29, **10%**	23.74
Pine (NO^+)	13.7, **65%**	nd	5.45, **26%**	1.83, **9%**	20.98 [10]

nd – no data

Figure 6: SIFT-MS selected ion mode/fast GC/SIFT-MS chromatograms for monoterpene emissions from pine tree samples (s1, s2 and s3) obtained using the MXT-Volatiles column. The upper and lower rows were obtained using H_3O^+ and NO^+ reagent ions respectively. The signal intensities are the analyte ion count rates normalized to a reagent ion count rate of 10^6 s^{-1}. The black and red curves stand for monitored ions $C_6H_9^+$ (m/z 81) and $C_{10}H_{17}^+$ (m/z 137) for H_3O^+ reagent ions of $C_7H_9^+$ (m/z 93) and $C_{10}H_{16}^+$ (m/z 136) for NO^+ reagent ions respectively. The last row shows calculated ratios of product ions r_i for both reagent ions (green and blue curves) and for peaks areas calculated $\overline{r_w}$ (red and black). The signal intensities are the analyte ion count rates normalized to a reagent ion count rate of 10^6 s^{-1}.

4.5 Comparison with previous studies

The present tests indicate that using the fast GC-SIFT-MS combination, it is possible to achieve analysis of the monoterpene mixture. The limit of detection was determined for α-pinene and R-limonene from analysis of a calibration curve as three times
5 the standard error of predicted intercept value divided by the slope of the calibration regression line (Graus et al., 2010). α-pinene and R-limonene were chosen as they have the lowest and the highest ration rate constants for proton transfer (2.3 for α-pinene and 2.6 for R-limonene, in $10^{-9} cm^3 s^{-1}$). When the reagent ion count rate was 10^6 c/s and 12 seconds sampling interval was used, the detection limit of the current setup was found to be 16.3 ppbv for α-pinene and 19.5 ppbv for R-limonene, using the column temperature 40 °C. For column temperature 69 °C, limit of detection for α-pinene decreased to 6.1 ppbv. This is
10 inferior to the previously described limit of the detection up to 1-2 ppb and full separation achieved by fastGC-PTR-MS systems (Materić et al., 2015; Pallozzi et al., 2016).

However, one advantage of SIFT-MS is the possibility to use another reagent ion as well as analysis of product ion ratios can be helpful. The combination of the data from the two reagent ions together with the analyses of the product ion signal ratios r_i can be shown to improve the identification of monoterpenes, especially identification of camphene and myrcene. It must be
15 kept in mind, that monoterpenes are not the only BVOCs emitted by plants. Especially when plants are physically damaged, they emit so called „leaf aldehydes" such as 2-, and 3-hexenal (Tani et al., 2003). Ion chemistry of these two aldehydes differs in SIFT-MS. Whilst the reaction of 2-hexenal with H_3O^+ proceeds as a proton transfer forming a product ion at m/z 99 (100 %), it has been found that reaction of cis-3-hexenal with H_3O^+ results in H_2O elimination producing a dominant fragment at m/z 81 (Španěl et al., 1997). To avoid an overlap of 3-hexenal with monoterpenes, it is thus more reliable to use the product ion at
20 m/z 137. Another possibility is to choose NO^+ as a precursor ion, where the product ions of 3-hexenal (m/z 97, 69 and 74) do not overlap with those of monoterpenes (m/z 92, 93 and 136) (Wang et al., 2003). Aside from potentially better selectivity, a benefit of employing the NO^+ regent ions in atmospheric analysis is quantification of isoprene, which for H_3O^+ regent ions interferes with furan, C5 aldehydes and 2-methyl-3-buten-2-ol (Karl et al., 2012; Karl et al., 2014), and overlapping with the second hydrate of methanol that is also emitted by plants (12% of global BVOC emissions) (Španěl et al., 1999). The same
25 approach can be applied to other isomeric or isobaric molecules present in environment. The last benefit of using SIFT-MS compare to other techniques is that calculation of VOC concentration in the sample depends only on the known physical constants, reaction rate constant and ions abundance. The system therefore does not require complicated calibration procedures. The results obtained from the analysis of leaf headspace samples in the terms of monoterpene composition agree well other studies in the published literature. Because the emission from plans depends on various physical parameters, here we compare
30 only monoterpene composition. In a previous study (Mumm et al., 2004) of the volatiles emitted by *Pinus nigra* needles, 35 terpenoid compounds were identified, with the following being most abundant: α-pinene (45%), β-phellandrene (9%), limonene (8%), β-pinene (5%) and 3-carene (2%). Holzke et al. (2006) studied diurnal and seasonal variation of monoterpenes and sesquiterpenes from Scots pine. The main isomers they observed were α-pinene, β-pinene and 3-carene, which represented

90% of the total terpene emission. A similar study on monoterpene emissions from boreal Scots pine showed that the most abundant monoterpenes measured above the forest and from the canopy were α-pinene and 3-carene (Räisänen et al., 2009). Kainulainen et al. (Kainulainen et al., 1992) investigated the effect of drought and waterlogging stress on needle monoterpenes of *Picea abies* (spruce). In the controlled group, the most abundant monoterpenes were camphene (22%), limonene (14%), α-pinene (9%) and myrcene (6%). In the emission from Southern and Central Sweden (Janson, 1993) the following isomers were most abundant: α-pinene (60-70%), camphene (10%), limonene (10%) and 3-carene (4%). Analysis of spruce samples (Zavarin et al., 1975) studied cortical oleoresin from *Abies concolor* (fir) that were collected in 43 different localities in order to analyse their composition for the monoterpenoid fractions. They concluded that the production of camphene and 3-carene varied geographically. In the study of (Pureswaran et al., 2004) they focused on quantitative variations in monoterpene vapours in four species of conifers, concluding that the four species (Douglas-fir, Lodgepole pine, Interior spruce and Interior Fir) did not differ qualitatively but there were significant differences in their quantitative profiles. For example, Coastal Douglas fir needle samples contained 10% of α-pinene, 31% of Sabinene and 40% of β-pinene, and in samples of interior Douglas fir the most abundant isomers were bornyl acetate (26%), camphene (25%), α-pinene and β-pinene (both 15%).

In presented study, we detected presence of α-pinene, β-pinene, camphene and 3-carene, representing common emissions emitted from pine, spruce and fir samples. The present results thus agree with the usually reported composition of terpenes emitted from pine trees and their parts.

5 Summary and conclusions

Addition of a fast GC pre-separation to SIFT-MS allows quantitative analyses of monoterpenes in mixtures at the expense of some loss of sensitivity. The bespoke electrically heated fast GC systems constructed for this study achieved separation in less than 45 s for a 5 m MXT-1 column and less than 180 s for a 5 m MXT-Volatiles column at 40 °C. The identification of monoterpenes was aided by using the information on the ratios of the product ion signals of both H_3O^+ and NO^+ reagent ions. It was shown that combining the SIFT-MS product ion ratios and the GC retention times 7 of 8 monoterpenes were identified in a mixture using the MXT-Volatiles column. To demonstrate analytical application of this novel combination of fast GC with SIFT-MS, volatile emissions from spruce, fir and pine samples were analysed. α-pinene was identified together with a lower amount of β-pinene and 3-carene. A significant contribution of camphene was also observed in the fir sample headspace. The fast GC SIFT-MS combination can thus be a step towards atmospheric analyses of monoterpenes that should resolve individual compounds due to their different reactivity with the OH radicals.

A weakness of the current fast GC setup is the relatively poor temperature stability caused by a strong dependence on the laboratory ambient temperature. However, this can surely be improved by active temperature feedback to control the column temperature. The flow rate through 5 m long and 0.28 mm i.d. column was about ten times lower than the conventional flow rate used in direct SIFT-MS analyses and this resulted in commensurate worsening of the limit of detection. This could be in future resolved by using a wider column or by using multiple capillaries in parallel. A clear advantage of SIFT-MS has been

shown to be in the possibility to use several different product ions to determine different fragmentation ratios from data obtained for H_3O^+ and NO^+ at the same retention time to improve the identification of compounds.

Data availability

All data are available upon request from the corresponding author (Michal Lacko).

5 **Author contribution**

ML and NW crated experimental hardwere and provided experiments with MXT-1 column, ML, KS and PP then provided experiments with MXT-Volatiles column. PS and ML provdided data reatment and paper preparation.

Competing interests

The authors declare that they have no conflict of interest.

15 **References**

Allardyce, R. A., Langford, V. S., Hill, A. L., and Murdoch, D. R.: Detection of volatile metabolites produced by bacterial growth in blood culture media by selected ion flow tube mass spectrometry (SIFT-MS), Journal of microbiological methods, 65, 361-365, 2006.

Amelynck, C., Schoon, N., and Dhooghe, F.: SIFT Ion Chemistry Studies Underpinning the Measurement of Volatile Organic
20 Compound Emissions by Vegetation, Current Analytical Chemistry, 9, 540-549, 2013.

Atkinson, R., Aschmann, SM., and Pitts Jr, JN.: Rate constants for the gas-phase reactions of the OH radical with a series of monoterpenes at 294±1 K. International Journal of Chemical Kinetics, 18, 287-299, 1986.

Atkinson, R., Aschmann, SM., and Arey, J.: Rate constants for the gas-phase reactions of OH and NO_3 radicals and O_3 with sabinene and camphene at 296±2 K. Atmospheric Environment Part A: General Topics, 24, 2647-2654, 1990.

Atkinson, R., Hasegawa, D., and Aschmann, SM.: Rate constants for the gas-phase reactions of O_3 with a series of monoterpenes and related compounds at 296±2 K, International Journal of Chemical Kinetics, 22, 871-887, 1990.

Atkinson, R., and Arey, J.: Gas-phase tropospheric chemistry of biogenic volatile organic compounds: a review, Atmospheric Environment, 37, S197-S219, 2003.

5   Chameides, W., Fehsenfeld, F., Rodgers, M., Cardelino, C., Martinez, J., Parrish, D., Lonneman, W., Lawson, D., Rasmussen, R., and Zimmerman, P.: Ozone precursor relationships in the ambient atmosphere, Journal of Geophysical Research: Atmospheres, 97, 6037-6055, 1992.

ChemicalBook: https://www.chemicalbook.com/ChemicalProductProperty_EN_CB4443087.htm, .

OriginPro 9.0 OriginLab Corporation, One Roundhouse Plaza, Suite 303, Northampton, MA 01060, United States. 1800-969-

10 7720.: https://www.originlab.com/, 2018.

Daubert, T. E.: Physical and thermodynamic properties of pure chemicals: Data compilation Hemisphere Pub. Corp., New York, 1989.

de Gouw, J., and Warneke, C.: Measurements of volatile organic compounds in the earth's atmosphere using proton-transfer-reaction mass spectrometry, Mass Spectrometry Reviews, 26, 223-257, 2007.

15 Ellis, A. M., and Mayhew, C. A.: Proton transfer reaction mass spectrometry: principles and applications, John Wiley & Sons, 2013.

Fehsenfeld, F., Calvert, J., Fall, R., Goldan, P., Guenther, A. B., Hewitt, C. N., Lamb, B., Liu, S., Trainer, M., and Westberg, H.: Emissions of volatile organic compounds from vegetation and the implications for atmospheric chemistry, Global Biogeochemical Cycles, 6, 389-430, 1992.

20 Garcia, G. A., Nahon, L., and Powis, I.: Near-threshold photoionization spectroscopy of the mono-terpenes limonene and carvone, International Journal of Mass Spectrometry, 225, 261-270, 2003.

de Gouw, J. A., Goldan, P. D., Warneke, C., Kuster, W. C., Roberts, J. M., Marchewka, M., Bertman, S. B., Pszenny, A. A. P., and Keene, W. C.: Validation of proton transfer reaction-mass spectrometry (PTR-MS) measurements of gas-phase organic compounds in the atmosphere during the New England Air Quality Study (NEAQS) in 2002, Journal of geophysical research:

25 atmospheres, 108, D21, 2003.

Graus, M., Müller, M., and Hansel, A.: High resolution PTR-TOF: quantification and formula confirmation of VOC in real time, Journal of the American Society for Mass Spectrometry, 21, 1037-1044, 2010.

Haynes, W. M.: CRC handbook of chemistry and physics, CRC press, New York, 2014.

Holzke, C., Hoffmann, T., Jaeger, L., Koppmann, R., and Zimmer, W.: Diurnal and seasonal variation of monoterpene and

30 sesquiterpene emissions from Scots pine (Pinus sylvestris L.), Atmospheric Environment, 40, 3174-3185, 2006.

Janson, R. W.: Monoterpene emissions from Scots pine and Norwegian spruce, Journal of geophysical research: atmospheres, 98, 2839-2850, 1993.

Jordan, A., Haidacher, S., Hanel, G., Hartungen, E., Herbig, J., Märk, L., Schottkowsky, R., Seehauser, H., Sulzer, P., and Märk, T. D.: An online ultra-high sensitivity Proton-transfer-reaction mass-spectrometer combined with switchable reagent ion capability (PTR+SRI−MS), International Journal of Mass Spectrometry, 286, 32-38, 2009.

Kainulainen, P., Oksanen, J., Palomäki, V., Holopainen, J., and Holopainen, T.: Effect of drought and waterlogging stress on needle monoterpenes of Picea abies, Canadian Journal of Botany, 70, 1613-1616, 1992.

Karl, T., Hansel, A., Cappellin, L., Kaser, L., Herdlinger-Blatt, I., and Jud, W.: Selective measurements of isoprene and 2-methyl-3-buten-2-ol based on NO^+ ionization mass spectrometry, Atmospheric Chemistry and Physics, 12, 11877–11884, 2012.

Karl, T., Kaser, L., and Turnipseed, A.: Eddy covariance measurements of isoprene and 232-MBO based on NO^+ time-of-flight mass spectrometry, International Journal of Mass Spectrometry, 365-366, 15-19, 2014.

Kesselmeier, J., and Staudt, M., Biogenic Volatile Organic Compounds (VOC): An Overview on Emission, Physiology and Ecology, Journal of Atmospheric Chemistry, 33, 23-88, 1999.

Kulmala, M., Suni, T., Lehtinen, K., Maso, M. D., Boy, M., Reissell, A., Rannik, Ü., Aalto, P., Keronen, P., and Hakola, H.: A new feedback mechanism linking forests, aerosols, and climate, Atmospheric Chemistry and Physics, 4, 557-562, 2004.

Lindinger, W., Hansel, A., and Jordan, A.: On-line monitoring of volatile organic compounds at pptv levels by means of proton-transfer-reaction mass spectrometry (PTR-MS) medical applications, food control and environmental research, International Journal of Mass Spectrometry and Ion Processes, 173, 191-241, 1998.

Malásková, M., Henderson, B., Chellayah, P., Ruzsanyi, V., Mochalski, P., Cristescu, S. M., and Mayhew, C. A.: Proton transfer reaction time-of-flight mass spectrometric measurements of volatile compounds contained in peppermint oil capsules of relevance to real-time pharmacokinetic breath studies. Journal of breath research, 2019.

Materić, D., Lanza, M., Sulzer, P., Herbig, J., Bruhn, D., Turner, C., Mason, N., and Gauci, V.: Monoterpene separation by coupling proton transfer reaction time-of-flight mass spectrometry with fast GC, Analytical and bioanalytical chemistry, 407, 7757-7763, 2015.

Matisová, E. and Dömötörová, M.: Fast gas chromatography and its use in trace analysis, Journal of Chromatography A, 1000, 199-221, 2003.

Mumm, R., Tiemann, T., Schulz, S., and Hilker, M.: Analysis of volatiles from black pine (Pinus nigra): significance of wounding and egg deposition by a herbivorous sawfly, Phytochemistry, 65, 3221-3230, 2004.

NIST WebBook Chemie, NIST Standard Reference Database Number 69, U.S. Secretary of Commerce, National Institute of Standards and Technology: Gaithersburg, MD: http://webbook.nist.gov/chemistry/ cited in January 2019.

Nolscher, A. C., Yanez-Serrano, A. M., Wolff, S., de Araujo, A. C., Lavric, J. V., Kesselmeier, J., and Williams, J.: Unexpected seasonality in quantity and composition of Amazon rainforest air reactivity, Nat Commun, 7, 10383, 2016.

Pallozzi, E., Guidolotti, G., Ciccioli, P., Brilli, F., Feil, S., and Calfapietra, C.: Does the novel fast-GC coupled with PTR-TOF-MS allow a significant advancement in detecting VOC emissions from plants?, Agricultural and Forest Meteorology, 216, 232-240, 2016.

Pureswaran, D. S., Gries, R., and Borden, J. H.: Quantitative variation in monoterpenes in four species of conifers, Biochemical systematics and ecology, 32, 1109-1136, 2004.

Pysanenko, A., Španěl, P., and Smith, D.: Analysis of the isobaric compounds propanol, acetic acid and methyl formate in humid air and breath by selected ion flow tube mass spectrometry, SIFT-MS, International Journal of Mass Spectrometry, 285, 42-48, 2009.

Räisänen, T., Ryyppö, A., and Kellomäki, S.: Monoterpene emission of a boreal Scots pine (Pinus sylvestris L.) forest, Agricultural and forest meteorology, 149, 808-819, 2009.

Rhoderick, G. C., and Lin, J.: Stability assessment of gas mixtures containing monoterpenes in varying cylinder materials and treatments, Analytical chemistry, 85, 4675-4685, 2013.

Rinne, J., Ruuskanen, T. M., Reissell, A., Taipale, R., Hakola, H., and Kulmala, M.: On-line PTR-MS measurements of atmospheric concentrations of volatile organic compounds in a European boreal forest ecosystem, Boreal environment research, 10, 425-436, 2005.

Romano, A., Fischer, L., Herbig, J., Campbell-Sills, H., Coulon, J., Lucas, P., Cappellin, L., and Biasioli, F.: Wine analysis by Fast GC proton-transfer reaction-time-of-flight-mass spectrometry, International Journal of Mass Spectrometry, 369, 81-86, 2014.

Savitzky, A., and Golay, M. J.: Smoothing and differentiation of data by simplified least squares procedures, Anal. Chem., 36, 1627-1639, 1964.

Schoon, N., Amelynck, C., Vereecken, L., and Arijs, E.: A selected ion flow tube study of the reactions of H_3O^+, NO^+ and O_2^+ with a series of monoterpenes, International Journal of Mass Spectrometry, 229, 231-240, 2003.

Shestivska, V., Antonowicz, S. S., Dryahina, K., Kubišta, J., Smith, D., and Španěl, P.: Direct detection and quantification of malondialdehyde vapour in humid air using selected ion flow tube mass spectrometry supported by gas chromatography/mass spectrometry, Rapid Communications in Mass Spectrometry, 29, 1069-1079, 2015.

Shestivska, V., Nemec, A., Dřevínek, P., Sovová, K., Dryahina, K., and Španěl, P.: Quantification of methyl thiocyanate in the headspace of Pseudomonas aeruginosa cultures and in the breath of cystic fibrosis patients by selected ion flow tube mass spectrometry, Rapid Communications in Mass Spectrometry, 25, 2459-2467, 2011.

Shestivska, V., Spanel, P., Dryahina, K., Sovova, K., Smith, D., Musilek, M., and Nemec, A.: Variability in the concentrations of volatile metabolites emitted by genotypically different strains of Pseudomonas aeruginosa, Journal of Applied Microbiology, 113, 701-713, 2012.

Smith, D., Španěl, P., Holland, T. A., Al Singari, W., and Elder, J. B.: Selected ion flow tube mass spectrometry of urine headspace, Rapid communications in mass spectrometry, 13, 724-729, 1999.

Smith, D., and Španěl, P.: Selected ion flow tube mass spectrometry (SIFT-MS) for on-line trace gas analysis, Mass spectrometry reviews, 24, 661-700, 2005.

Smith, D., and Španěl, P.: Ambient analysis of trace compounds in gaseous media by SIFT-MS, Analyst, 136, 2009-2032, 2011a.

Smith, D., and Španěl, P.: Direct, rapid quantitative analyses of BVOCs using SIFT-MS and PTR-MS obviating sample collection, TrAC Trends in Analytical Chemistry, 30, 945-959, 2011b.

Smith, D., Sovová, K., and Španěl, P.: A selected ion flow tube study of the reactions of H_3O^+, NO^+ and $O_2^{+\bullet}$ with seven isomers of hexanol in support of SIFT-MS, International Journal of Mass Spectrometry, 319, 25-30, 2012.

5 Song, M., Xia, Y., and Tomasino, E.: Investigation of a Quantitative Method for the Analysis of Chiral Monoterpenes in White Wine by HS-SPME-MDGC-MS of Different Wine Matrices, Molecules, 20, 7359-7378, 2015.

Španěl, P., Ji, Y., and Smith, D.: SIFT studies of the reactions of H_3O^+, NO^+ and O_2^+ with a series of aldehydes and ketones, International journal of mass spectrometry and ion processes, 165, 25-37, 1997.

Španěl, P., and Smith, D.: Selected ion flow tube studies of the reactions of H_3O^+, NO^+, and O_{2+} with several aromatic and

10 aliphatic hydrocarbons, International Journal of Mass Spectrometry, 181, 1-10, 1998.

Španěl, P., Davies, S., and Smith, D.: Quantification of breath isoprene using the selected ion flow tube mass spectrometric analytical method, Rapid communications in mass spectrometry, 13, 1733-1738, 1999.

Španěl, P., Dryahina, K., and Smith, D.: A general method for the calculation of absolute trace gas concentrations in air and breath from selected ion flow tube mass spectrometry data, International Journal of Mass Spectrometry, 249-250, 230-239,

15 2006.

Španěl, P., and Smith, D.: Advances in On-line Absolute Trace Gas Analysis by SIFT-MS, Curr. Anal. Chem., 9, 525-539, 2013.

Takasago: http://www.takasago.com/cgi-bin/pdf/alphaterpinene.pdf, 2011, cited in January 2019.

Tani, A., Hayward, S., and Hewitt, C.: Measurement of monoterpenes and related compounds by proton transfer reaction-mass

20 spectrometry (PTR-MS), International Journal of Mass Spectrometry, 223, 561-578, 2003.

TGSC, The Good Scents Company Information System: http://www.thegoodscentscompany.com/, cited in January 2019.

Thompson, J. M., and Perry, D. B.: A new system of refillable and uniquely identifiable diffusion tubes for dynamically generating VOC and SVOC standard atmospheres at ppm and ppb concentrations for calibration of field and laboratory measurements, Journal of Environmental Monitoring, 11, 1543-1544, 2009.

25 Van Kempen, G. M. P., and Van Vliet, L. J.: Mean and variance of ratio estimators used in fluorescence ratio imaging, Cytometry Part A, 39, 300-305, 2000.

Wang, T., Španěl, P., and Smith, D.: Selected ion flow tube, SIFT, studies of the reactions of H_3O^+, NO^+ and $O2^+$ with eleven $C_{10}H_{16}$ monoterpenes, Int. J. Mass Spec., 228, 117-126, 2003.

Yaws, C. L.: Handbook of Vapor Pressure. Vol 3: C8-C28 Compounds, Gulf Pub Co., Houston, 1994.

30 Zavarin, E., Snajberk, K., and Fisher, J.: Geographic variability of monoterpenes from cortex of Abies concolor, Biochemical Systematics and Ecology, 3, 191-203, 1975.